

Is it Truly Necessary for Bicycle Power Meters to Rapidly Sample Angular Velocity?

Jack Renshaw - The University of New South Wales

June 17, 2024

Abstract

Bicycle Power Meters have become ubiquitous in professional and amateur cycling. These devices claim high levels of accuracy, and this accuracy is indeed essential if they are to serve their purpose as reliable training aids and indicators of improvements in fitness. Power is generally obtained via the independent estimation of torque and angular velocity. Designs vary in the way in which they estimate angular velocity. Some power meters estimate angular velocity many times a second, whereas other power meters compute an average value for each pedal stroke. The aim of this paper is to investigate whether it is necessary to rapidly sample angular velocity in order to obtain accurate power values under conditions of dynamic equilibrium. Countering previous research on the topic, this paper finds that average angular velocity alone is usually sufficient for the purposes of computing power, although there may be certain exceptional circumstances where consideration of harmonics may appreciably improve fidelity.

Contents

1	Introduction	2
1.1	Power Meters in Amateur and Professional Cycling	2
1.2	Literature Review	2
1.3	The Operation of Bicycle Power Meters	3
1.3.1	Instantaneous Angular Velocity (IAV)	3
1.3.2	Average Angular Velocity (AAV)	3
1.3.3	Theoretical Case for Power Error	4
2	Analysis of Favero Study and Dataset	5
2.1	Test Subset	6
2.2	Conclusion	6
3	Dynamic Model of a Cyclist	7
3.1	A Mechanical and Kinematic Model of a Bicycle-Rider System	7
3.1.1	Indoor Bicycle Trainers	7
3.2	A Cyclist in Dynamic Equilibrium	8
3.2.1	Force and Acceleration	8
3.3	Power, Averaging, and Oscillations in Velocity and Force	8
3.3.1	Cross-Correlation Error	8
3.3.2	Non-Conservative Forces and Jensen's Inequality	9
3.4	A Mathematical Model of the Pedal Stroke	9
3.4.1	An Empirical Model of the Pedal Stroke	9
3.4.2	Induced Variations in Angular Velocity	10
3.5	System Modelling	11
3.5.1	Harmonic Losses in RL Circuits with multiple harmonics and a DC Offset	12
3.5.2	Unilateral Torque Measurement	13
3.5.3	A Tangential Comment on Dynamic Inequilibrium	14
4	Model Validation and Extrapolation	15
4.0.1	Model Fidelity	15
4.1	Simulations	16
4.1.1	AV Variation and Power Error	16
5	Conclusion	18

1 Introduction

In his preface to *Electromagnetic Waves*, Sergei Schelkunoff noted that theoretical physicists have a tendency to "lose sight of the interdependence of force and velocity waves" when considering the propagation of the eponymous waves through various media, and that the engineering approach, which was to "introduce the second important wave concept, that of the impedance", proved to be of significance in physics as well as engineering.

When designing electromechanical devices that aim to accurately estimate power, the product of force and velocity, it is no less important to consider, in a concrete fashion, the mechanical characteristics of the power producing system and characteristics of the medium through which the system moves. This paper will suggest that an appropriate analytical framework for modelling such systems and their environment is via an electrical analogue, thereby leveraging the concept of impedance and the plethora of techniques and simulation tools available to electrical engineers. Prudent consideration of the impedance of the system of interest is necessary to ensure that power estimating devices perform, and to ensure that they are not over-engineered.

This paper will focus on the estimation of mechanical power by bicycle *Power Meters*, however the framework and methodology utilised by this paper is applicable to a number of situations beyond this particular context. In contrast to previous research on the topic, this paper concludes that, under most circumstances, the mechanical and biomechanical characteristics of the typical cyclist are such that the rapid sampling of angular velocity is not necessary to obtain highly accurate power estimates; accurate power estimates can be obtained by considering only the average angular velocity throughout the pedal stroke. This result derives from the fact that cyclists have high inertia. Even when variations in velocity or force are high, this inertia tends to result in the principal harmonic components of force and velocity co-existing in quadrature, and they therefore make no meaningful contribution to mechanical work.

1.1 Power Meters in Amateur and Professional Cycling

Bicycle Power Meters have become a mainstay of effective training for professional and amateur cyclists. These devices aim to estimate the mechanical power delivered by the rider to the bicycle and ultimately to forward propulsion. The purpose of estimating power is to deliver an objective measure of performance to a sport that is confounded by complicating environmental variables. An ideal power meter would measure and report the power applied to the pedal at every point. As it is not possible to measure power directly, power is usually estimated via the independent estimation of force and velocity. Power meters generally function by estimating torque via the use of strain gauges, and estimating angular velocity either via the measurement of rotational period, or centripetal acceleration. These quantities are related by the following equation:

$$P = \tau \times \omega \quad (1)$$

Power is typically calculated over the period of a single pedal stroke, which is the period (T henceforth) over which the bicycle crank traces an entire revolution. Torque and angular velocity may be sampled spatially or temporally. Properly computed, the average power over this period is:

$$P_{avg} = \frac{1}{T} \int_0^{2\pi} \tau(\theta) \times \omega(\theta) d\theta = \frac{1}{T} \int_0^T \tau(t) \times \omega(t) dt \quad (2)$$

1.2 Literature Review

This paper is largely a response to, and critique of, a research paper published by Favero[3]. Favero is a manufacturer of a popular power meter, the *Assioma*. One crucial differentiating feature of the *Assioma* in relation to other power meter models is *Instantaneous Angular Velocity* (IAV), which is essentially a high rate of sampling angular velocity; a feature achieved through the use of gyroscopes. The Favero Paper seeks to justify the supremacy of this design choice, and contains two aspects:

1. A theoretical discussion of how pedal stroke variation might give rise to error in the computation of power.
2. Analysis of experimental data that supposedly demonstrates that fact.

Favero's Paper concluded that not considering variations in angular velocity could account for errors "as high as -1.6% using round chainrings and +4.5% using oval chainrings" and that "different patterns were also observed depending on the type of indoor trainer used".

Danek et Al, 2022[2] expanded upon the brief theoretical explanation provided by Favero with deeper analysis, and then provided a numerical example which indicated that there existed

a discrepancy between the power-meter calculations resulting from the use of the instantaneous-pedal-speed and average-pedal-speed information. Removing this discrepancy is crucial for a variety of information that rely on power measurements, as is the case of this article.

Danek et Al stated that "neglecting speed variation during a pedal stroke" produced a "different - and less accurate" power result.

This paper will introduce three primary criticisms of the Favero Paper on *Methodological*, *Inferential* and *Theoretical* grounds. These critiques are based on what this paper finds to be the errant conclusion of the Favero Paper, which is that:

variation of angular velocity within a rotation has a considerable impact on the error in calculation of any algorithm that does not take it into account.

This claim implies a causal relationship between angular velocity variation and power error. The paper further claims that:

all cycling conditions that produce an increase in the unevenness of rotational speed within the pedal stroke progressively influence the error in the calculation of power; these conditions depend on the equipment used (chainrings), cycling situation (on trainer or road, flat road or climb), as well as the pedaling style of each cyclist.

The use of "progressive" implies a 'dose-response' relationship between angular velocity variation and power error. The primary empirical basis for this claim is the "high correlation coefficient [of] $R^2 = 0.93$ " between Angular Velocity and Power Error. The Paper also states that:

only signals relevant to the left pedal were aquired

However, Favero's Paper also claims that:

all the following considerations [related to power error being produced by variation in angular velocity], although referring to the pedal, remain valid even when the points at which the moment of force M and the rotational speed ω are detected are situated on the crank arm or spider or on the bottom bracket/hub.

While it is true in the strictest sense that AV Variation is necessary for power error to occur, this paper will argue that it is neither causal (i.e, AV Variation is the by-product of system dynamics, and it is the system dynamics that give rise to power error if and where it exists), nor is AV Variation alone sufficient to produce meaningful power error. Furthermore, this paper will argue that power error observed by Favero's Paper under certain scenarios was a side effect of the test design (specifically the choice to compute power unilaterally - refer to Section 3.5.2), and quantative conclusions in relation to power error cannot be generalised to most power meters, which measure power bilaterally.

1.3 The Operation of Bicycle Power Meters

This paper will adopt Favero's Paper's functional categorisation of techniques for measuring angular velocity for the purposes of computing power; IAV and AAV. These techniques are outlined below.

1.3.1 Instantaneous Angular Velocity (IAV)

Power Meters that rapidly sample angular velocity typically utilise multiple gyroscopes or accelerometers to estimate angular velocity instantaneously, usually at the same rate at which strain is sampled. Power under the scheme of IAV can be computed by taking the average value of the product of the constituent terms:

$$P_{avg} = \frac{1}{N} \sum_{t=1}^N \tau[t]\omega[t] \quad (3)$$

1.3.2 Average Angular Velocity (AAV)

Some power meters utilising AAV perform an averaging of sampled angular velocity over the course of the pedal stroke, whereas other designs only have the ability to determine angular period. The general scheme of AAV-based power measurement is shown in Figure 1. Essentially, torque τ is sampled at a high rate, and a time-difference is computed for the length of a pedal stroke.

The combination of time and torque measurements result in an "average" power figure via homogenously weighting every sample of torque taken:

$$P_{avg} = \frac{\sum_{t=0}^N \tau_t}{N * (T_0 - T_{-1})} \quad (4)$$

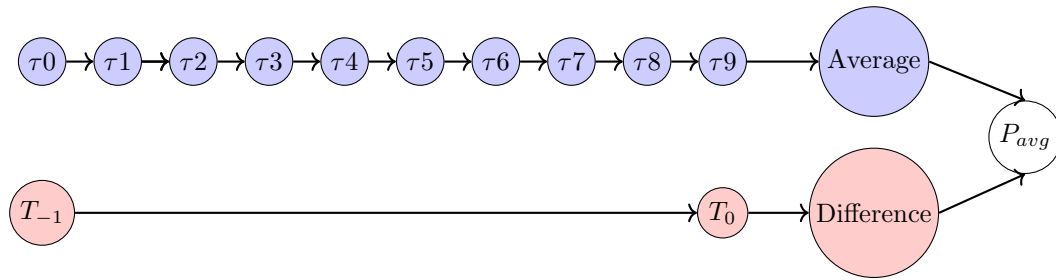


Figure 1: System model for the measurement of power via AAV

1.3.3 Theoretical Case for Power Error

As indicated by the Favero Paper, the AAV technique neglects any consideration of angular velocity variation throughout the pedal stroke. Specifically, this technique assumes either no variation in angular velocity throughout the pedal stroke, or that if there is angular velocity variation, it is uncorrelated with the application of torque. Favero's argument that this will produce power error is summarised as follows:

Power can be expressed as the cross-product of torque (τ) and angular velocity (ω), which vary in time.

$$P(t) = \tau(t) \times \omega(t)$$

Both τ and ω "can be expressed as a Fourier series of sine waves (harmonics) extending by periodicity a single period"¹. For simplicity, τ and ω will be treated as scalar quantities by considering only rotation about the crank spindle. A substitution of the Fourier Series of these signals into the power equation yields:

$$\begin{aligned}
 P(t) &= \tau_0 * \omega_0 + \\
 &\tau_0 * \sum_{n=1}^{\infty} \omega_n \cos\left(\frac{2\pi n t}{T} + \theta_n\right) + \\
 &\omega_0 * \sum_{k=1}^{\infty} \tau_k \cos\left(\frac{2\pi k t}{T} + \phi_k\right) + \\
 &\sum_{n=1}^{\infty} \sum_{k=1}^{\infty} \tau_k * \omega_n * \cos\left(\frac{2\pi n t}{T} + \theta_n\right) * \cos\left(\frac{2\pi k t}{T} + \phi_k\right)
 \end{aligned}$$

Power error derives from the final double-sum term², as the preceding terms evaluate to zero when integrated over the period of the pedal stroke. The Favero Paper also notes the following:

1. The contribution of harmonics (of the same order with each other) is zero when they are in quadrature.
2. Angular velocity tends to have a dominant harmonic twice the fundamental frequency.
3. It is not possible to establish a priori whether the harmonics can increase or decrease the result obtained from the average values.

The primary critique of this theoretical argument is that the relationship between torque and angular velocity is decontextualised when circular chainrings are used. Under the conditions implied, where the 'periodicity of a single pedal stroke is [smoothly] extended', variations in angular velocity are *induced* by variations in applied torque, and it is in fact possible to make reasonable predictions about both the sign and magnitude of power error. Specifically:

1. The fact that angular velocity lags force (by at most quadrature), means that AAV will necessarily under-predict power. Power Error will thus be strictly negative³.
2. Cyclists tend to have high inertia, so harmonics of the same order are usually in approximate quadrature.
3. By the fact of 2, power error under conditions thus described is generally very small.
4. When inertia is low, for example on an indoor trainer, power error may genuinely be elevated.

¹This claim makes the unstated assumption that the Fourier Series of the constructed periodic signal converges, which assumes smoothness. As will be discussed in a later section, this implies conditions of dynamic equilibrium

²The Paper performed a trigonometric substitution to reduce the double-sum to a single-sum

³Adopting Favero's convention for error sign

2 Analysis of Favero Study and Dataset

A flaw in the Favero Paper stems from the improper treatment of collected data, the theoretical and methodological limitations noted above notwithstanding. The authors misinterpreted the collected data by drawing a false continuity between the angular velocity variation induced by ovalised chainrings and that induced by circular chainrings, thereby attributing power error induced by another aspect of ovalised chainrings (namely, a changed phase-angle relationship) to the increased variation in angular velocity which is a side-effect of ovalised chainrings. The Favero Paper's dataset provided in the study was entered into Python for reanalysis, producing a near-identical result. A strong Cubic relationship between angular velocity variation and power error is visible. The data was also reanalysed using a Linear Fit.

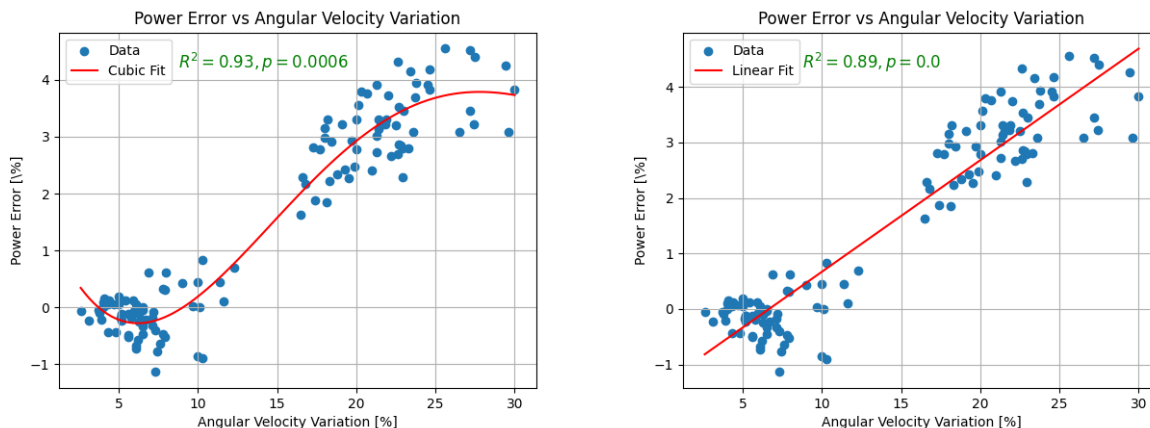


Figure 2: Cubic and Linear Fits of Favero Paper dataset

Clearly, there is a strong and statistically significant linear correlation between angular velocity variation and error. Notably, this aggregate dataset combines two categorically distinct datasets, tests that utilise non-circular (ovalised) chainrings, and tests that utilise circular chainrings. The datasets were analysed separately below. For tests that utilise circular chainrings, the focus of this paper, there is no statistically significant correlation between angular velocity variation and error.

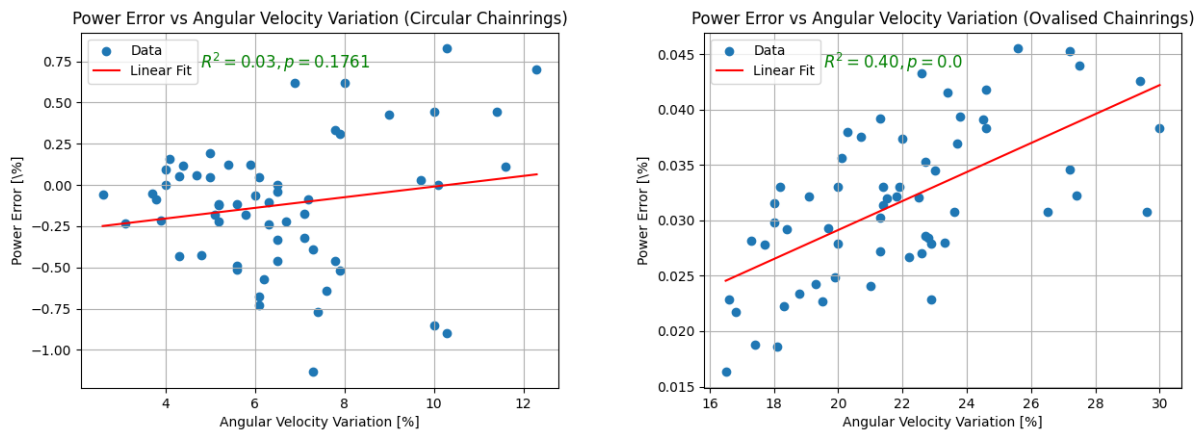


Figure 3: Separately Considered Linear fit of Circular and Ovalised Chaining Datasets

When a Linear fit is applied to *Absolute Error* for the circular chaining subset of tests, the relationship is small and statistically significant. There is no individual test where a statistically significant relationship between angular velocity variation and absolute error emerges. This is evident in a randomly selected test (*T2.2.2*), where a statistically significant **negative error** exists between the two variables, bucking the trend within the *T2.X.X* dataset of a positive error relationship.

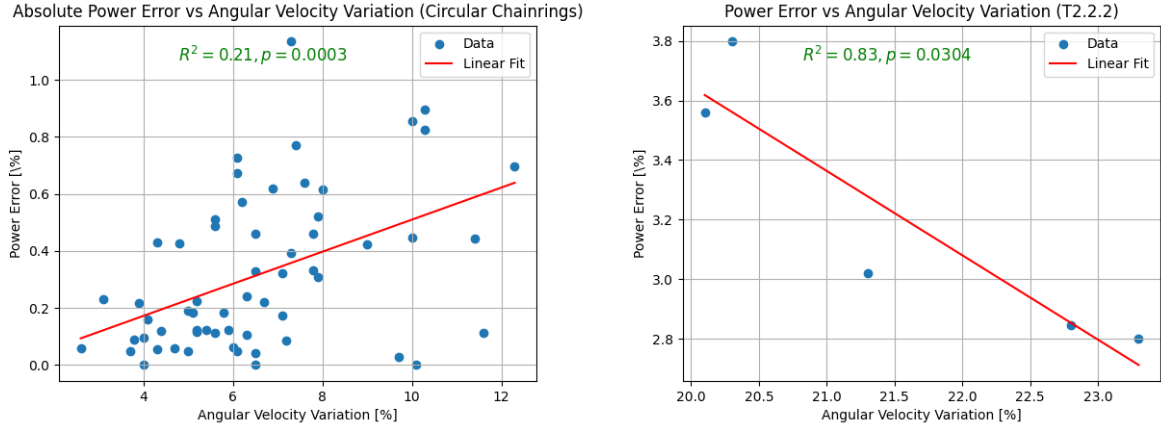


Figure 4: Linear Fit of Circular Chainring dataset and T2.2.2

A causal relationship between Angular Velocity Variation and Power Error cannot be claimed. The spurious presence of a strong relationship is the result of Hidden Variables. The postulated hidden variable present in this dataset is phase relationship; ovalised chainrings, by their very nature, introduce a phase relationship between torque and angular velocity that is unrelated to system dynamics, is not in quadrature with torque, and thus results in a degree of correlation between AV Variation and Torque.

2.1 Test Subset

A subset of the Paper's results, shown in Table 5 in the Annex, were selected for further analysis. Specifically selected were those tests that utilise circular chainrings and where parameters such as equivalent mass and cadence were known or could be estimated. This subset of tests was used to generate a cross-correlation matrix visible in Table 1, with concomitant p-values visible in Annex A, Table 6. Three synthetic parameters were generated - Absolute Error ($E2$) = $\sqrt{E^2}$, Force = $\frac{IAV}{RPM}$, and FMR = $\frac{Force}{Mass}$.

	Mass	Grade	RPM	Var	IAV	AAV	Force	FMR	E	E2
Mass	1.00	0.73	-	-	-	-	-	-0.91	0.71	-0.40
Grade	0.73	1.00	-0.49	-	-	-	0.39	-0.65	0.63	-
RPM	-	-0.49	1.00	-0.59	-0.58	-0.53	-0.88	-	-0.09	-0.44
Var	-	-	-0.59	1.00	-	-	0.49	-	-	0.45
IAV	-	-	-0.58	-	1.00	0.95	0.87	0.40	-	0.66
AAV	-	-	-0.53	-	0.95	1.00	0.79	0.48	-0.35	0.66
Force	-	0.39	-0.88	0.49	0.87	0.79	1.00	-	-	0.59
FMR	-0.91	-0.65	-	-	0.40	0.48	0.19	1.00	-0.85	0.65
E	0.71	0.63	-	-	-	-0.35	-	-0.85	1.00	-0.71
E2	-0.40	-	-0.44	0.45	0.66	0.66	0.59	0.65	-0.71	1.00

Table 1: Subset Correlations

Of the non-trivial correlations between dependant and independent variables, Force to Mass Ratio (FMR) has the strongest correlation with signed error. Higher FMR results in AAV underestimating power vis à vis IAV. There is a moderate and statistically significant relationship between Absolute Power Error and Mass, Cadence (RPM), Variation, Force and FMR.

2.2 Conclusion

The outcome of this section is that the Paper's empirical dataset is not sufficient to draw any firm, causal conclusions about the relationship between angular velocity variation and power meter error. For example, the amount of power itself appears to be a stronger predictor of power error than AV Variation. This implies that AV Variation is a side effect of a deeper phenomenon that results in power error.

The following section will demonstrate that AV Variation, despite being a necessary condition for power error to exist, is not alone sufficient due to the fact that angular velocity is usually in approximate quadrature with net applied torque.

3 Dynamic Model of a Cyclist

The section will outline the model used for characterising the behaviour of a *Bicycle-Rider System* (BRS) within a single pedal stroke. The behaviour of interest involves small accelerations and decelerations that produce no net change in velocity over the course of the period. Environmental conditions (grade, the relative velocity of the wind, etc) are assumed to remain constant throughout this time period - the BRS is in a state of *Dynamic Equilibrium*. This model will be developed by first outlining a mechanical and kinematic model of a cyclist under conditions of dynamic equilibrium as defined, and then deriving expressions for acceleration in terms of the parameters of the BRS and opposing forces. An Electrical Analogy of the BRS will be introduced, which will serve as the basis of the modelling which will be performed in Section 4.

3.1 A Mechanical and Kinematic Model of a Bicycle-Rider System

The application of force to the pedal of a bicycle is transferred via a number of mechanical connections into torque applied at the contact patch of the rear tyre to the road, which results in the BRS applying a net force against external impeding forces. The BRS has inertia and drag, and the tyres have rolling resistance. Cycling up a hill requires a force to be applied against gravity. A cyclist travelling at v and up a gradient with angle θ is subject to wind resistance, a quadratic function of the BRS wind velocity difference, and a force due to gravity:

$$F_t = F_d + F_g = \frac{1}{2}\rho CdA * (v - v_{wind})^2 + mgsin(\theta) \quad (5)$$

Where:

v Is the linear velocity of the bicycle-rider system with respect to the ground.

v_{wind} Is the average velocity of the wind with respect to the ground.

m Is the mass of the entire bicycle-rider system.

g Is the gravitational constant.

ρ Is air density.

Cd Is the coefficient of drag of the entire system.

A Is the frontal surface area of the entire system.

The average power required to maintain this velocity, assuming velocity remains constant, is given by:

$$P_{avg} = \omega_{avg} \int_0^T \tau(t) dt = v_{avg} \int_0^T F(t) dt = \frac{1}{2}\rho CdA(v_{avg} - v_{wind})^3 + vmgsin(\theta) \quad (6)$$

There are also some frictional forces present resulting from the chain, bearings, and tyres on the road. Frictional forces tend to be linear with velocity; however there may be some dependance on both ω and v . These forces are usually small, and will be ignored for the purposes of this paper. For the purposes of this paper, a linear approximation will be taken for all resistive forces, which gives rise to the following equation of motion:

$$F = mg \sin(\theta) + k\dot{x} + m\ddot{x} \quad (7)$$

3.1.1 Indoor Bicycle Trainers

Indoor Bicycle Ergometers (also called Bicycle Trainers) have become popular in recent years. There are a number of schemes employed to provide resistance to the cyclist. These include fluid resistance, fan-driven resistance, and magnetic resistance. This paper considers magnetic resistance, the form of resistance utilised by the Elite Quobo Trainer in Favero's Paper. Bicycle Trainers mimic the inertia of a cyclist via the use of a flywheel. For simple magnetic trainers operating in their linear region, the resistive force generated by Eddy Currents circulating in the trainer flywheel can be derived via an application of Lenz's Law:

$$\epsilon = -N \frac{\partial \phi_B}{\partial t} \quad (8)$$

Where $\frac{\partial \phi_B}{\partial t}$ is generally $\propto \omega_{flywheel}$. It is possible to linearise the dynamics of this rotating system by equating $\omega_{flywheel}$ with linear velocity v , converting moment of inertia into equivalent mass ($m = kI$), and considering magnetic resistance to be linearly velocity-dependant. This produces the same fundamental of motion as the linear motion of a cyclist outdoors:

$$F = C_m \dot{x} + M_{eq} \ddot{x} \quad (9)$$

3.2 A Cyclist in Dynamic Equilibrium

A cyclist's velocity on a bicycle ride, $v(t)$ ⁴, will contain some amount of variation. The angular velocity of the pedal, $\omega(t)$, will also vary and, in a constant gear, $v(t) \propto \omega(t)$ ⁵. This paper distinguishes between two types of variation in velocity:

1. **Oscillations**, which are periodic variations in velocity that are contained within a single pedal stroke.
2. **Accelerations**, which are net changes in velocity from the start to the end of a pedal stroke.

If net acceleration over some time period T (the length of a pedal stroke) is zero, then a cyclist is in *Dynamic Equilibrium* over that period. The mathematical condition for dynamic equilibrium is

$$\int^T \frac{dv(t)}{dt} = \int^T \frac{d\omega(t)}{dt} = 0 \quad (10)$$

Under conditions of dynamic equilibrium, any change in velocity during T (but not over T , for there is no change over T by construction) is purely a product of a previous change in force. If a cyclist is in a dynamic equilibrium for period T , it is possible to redefine $v(t)$ as a periodic function (with period T) by extending the definition of $v(t)$ to $t \in \mathbb{R}$ such that $v(t)$ satisfies the condition that, for $a \in \mathbb{Z}, t \in [0, T], v(t) = v(aT + t)$. $v(t)$ is a smooth function by construction⁶, and finite due to the fact that it represents a real quantity of only finite values. Given $v(t)$ is smooth and finite, bounded variation can be asserted which is the condition of the Dirichlet–Jordan test, and the Fourier Series $S_n(v(t))$ converges to $v(t)$.

3.2.1 Force and Acceleration

Force and Acceleration are not necessarily smooth time-varying quantities, however in physical systems they are finite-valued. A differential equation for acceleration can be derived by expressing force as a Fourier Series⁷ and utilising a linear approximation of opposing forces.

$$\frac{dv(t)}{dt} = \frac{1}{m} (F_0 + \sum_{n=1}^{\infty} F_n \sin(2\pi nt + \phi_n) - kv - mg \sin(\theta)) \quad (11)$$

The periodicity of force application coincides with the periodicity of velocity, since changes in velocity are entirely driven by the periodic application of force (and the monotonically increasing impeding function)⁸. Because the gear-ratio is assumed to remain constant, for $t \in [0, T], v \propto \omega$ and $\tau \propto F$ ⁹.

3.3 Power, Averaging, and Oscillations in Velocity and Force

A primary aim of this paper is to explore how oscillations in linear or angular velocity might contribute to differences in the power produced and measured in a state of dynamic equilibrium when differing techniques for computing power, Average Angular Velocity (AAV) and Instantaneous Angular Velocity (IAV), are employed. There are two theoretical sources of error that might result from averaging angular velocity.

3.3.1 Cross-Correlation Error

Torque and Angular Velocity can be described as a quantities that continuously vary in time - $\tau(t)$ and $\omega(t)$ - from which it is possible to calculate $P(t) = \tau(t) \times \omega(t)$. If we are interested in the average power, labelled \bar{P} , over some period T we will not arrive at a precise result by considering the product of the averages of the individual components, $\bar{\tau} * \bar{\omega}$, due to the precense of **cross-correlation**. For two differentiable functions, f and g , it is generally the case that:

$$\int f(x)g(x) dx \neq \int f(x) dx \int g(x) dx \quad (12)$$

Cross-Correlation Error could be either positive or negative, depending on the sign of the cross-correlation between the two functions under consideration.

⁴Velocity and concomitant quantities are treated as scalar

⁵This is assuming that bicycle gears are perfectly stiff and circular, that force and velocity are seamlessly transferred from the pedal to the rear wheel.

⁶ $v(t)$ is smooth by construction due to the fact that, for $a \in \mathbb{Z}$, the limit of $v(aT + t)$ as $t \rightarrow T$ (and $\therefore aT + 1 \rightarrow (a + 1)T = v((a + 1)T)$ by virtue of the extended definition of $v(t)$

⁷As will be discussed in the following section, it is empirically true that force can be expressed as a Fourier Series and can be well-approximated with a small number of terms

⁸This claim is not proven explicitly, however it is self evidently true in the case of the electrical analogue introduced later

⁹The relationship between $\tau \& F$ and $\omega \& v$ is through power balance $\tau \times \omega = F * v$; $\omega(t) = k_0 v(t)$ and $\tau(t) = k_1 F(t)$

3.3.2 Non-Conservative Forces and Jensen's Inequality

There is a third order polynomial relationship that characterises the relationship between velocity and power. A realistic example of this relationship is shown in Figure 5. This relationship between velocity and the power required to maintain that velocity[6] means that oscillations or variations about an average velocity value result in higher average power requirements for a given average speed, and the greater the variance in velocity, the greater the average power requirements for the same speed. This is due to Jensen's inequality; in Figure 5, the size of the projection of the secant line connecting V_0 and V_+ onto the Power-Axis is greater than the same projection of the secant line connecting V_0 and V_- .

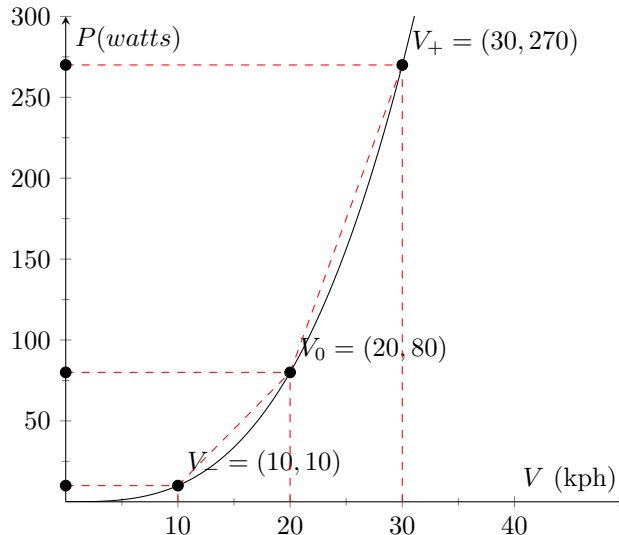


Figure 5: An illustration of how Jensen's Inequality may contribute to reported power error.

For the purposes of illustration, consider the power computed by averages and properly for a cyclist travelling 20km during the course of one hour in an oscillatory fashion. Specifically, the cyclist travels at 30kph (270W) for 30 minutes and then 10kph(10W) for the remainder. AAV would predict an average power of 80W (20kph), whereas IAV would produce an average power of 140W (neglecting accelerations).

3.4 A Mathematical Model of the Pedal Stroke

The cycling pedal stroke is characterised by the application of torque by the cyclist. The application of torque is quasiperiodic; that is, there is a regular variation within pedal strokes, but also some level of variation over longer time periods (due to changes in gear, gradient, decisions to accelerate or decelerate). This section shall characterise the variation in force application within a single pedal stroke.

3.4.1 An Empirical Model of the Pedal Stroke

Bini & Carpes, 2014[1] measured the force exerted by a certain cyclist on a pedal throughout the course of a single pedal stroke, with results presented in Figure 6. This pedal stroke will be characterised and used as the basis for simulation. The pedal stroke developed is one particular pedal stroke, and there likely some amount of variation between cyclists, as well as variation across different conditions and with fatigue. In spite of this fact, this pedal stroke does contain non-idealities which are potential contributing factors to power error, such as an imbalance between left and right torque application¹⁰.

Temporal variation in torque was analysed in terms of its frequency content¹¹, and harmonics are presented in terms of their amplitude and phase angle in Table 2. Harmonics above the fifth were omitted for the sake of brevity.

Total Harmonic Distortion (THD) was calculated with respect to the DC content of the pedal stroke.

$$THD(\%) = \frac{\sqrt{\sum_{i=1}^5 V_i^2}}{V_0} \quad (13)$$

¹⁰The results of this paper could be more strongly claimed with a thorough empirical model of the pedal stroke

¹¹Using a Discrete Fourier Transform (DFT)

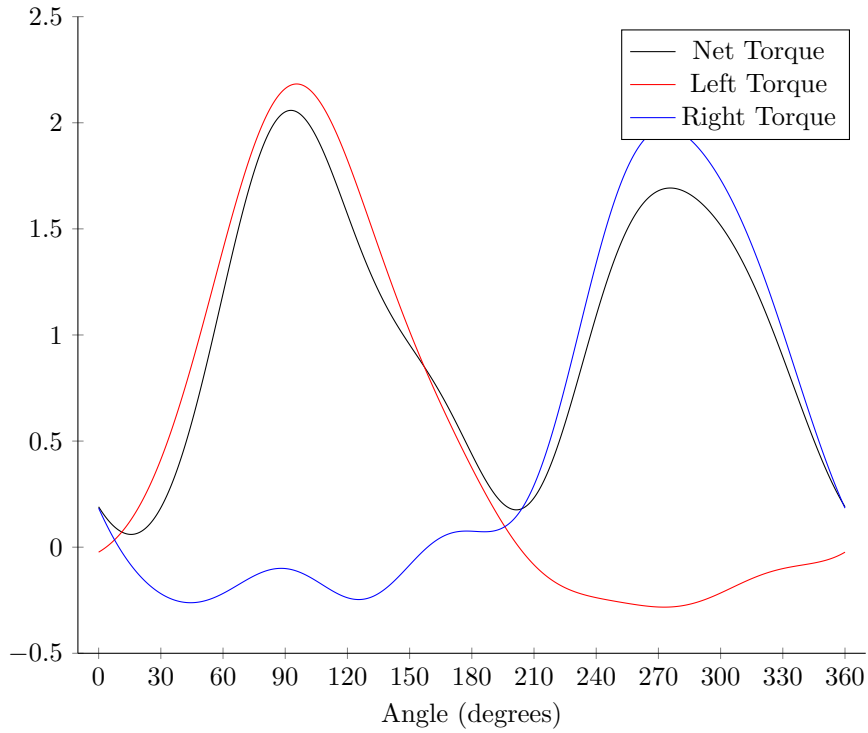


Figure 6: Variations in Applied Torque

	Net Torque	Left Torque	Right Torque
DC Component	1.000 \angle - 0.000	0.521 \angle - 0.000	0.479 \angle - 0.000
1st Harmonic	0.099 \angle - 121.386	1.089 \angle - 99.993	0.997 \angle 82.088
2nd Harmonic	0.849 \angle 157.439	0.410 \angle 158.783	0.439 \angle 156.185
3rd Harmonic	0.079 \angle 129.510	0.137 \angle 89.984	0.091 \angle - 123.439
4th Harmonic	0.127 \angle 45.443	0.042 \angle 29.845	0.088 \angle 52.782
5th Harmonic	0.045 \angle - 118.745	0.014 \angle - 43.564	0.044 \angle - 137.366
<i>THD</i> (%)	193%	284%	287%

Table 2: Normalised Harmonic Content of a Typical Pedal Stroke

It should be noted that there is an upper limit on the amount of THD that could realistically be present in a pedal stroke, due to the fact that the freehub ratchet prevents the application of negative torque to the rear wheel. Future work could involve determining an upper limit on power error based on this physical limitation, as opposed a single empirical model of a pedal stroke.

3.4.2 Induced Variations in Angular Velocity

Variations in net torque give rise to variations in Angular Velocity. This is represented below considering only the dominant harmonic of angular velocity; observe the phase relationship between torque and angular velocity. That is, angular velocity *lags* the application of torque due to the fact that torque variation *induces* angular velocity variation. For reasons that will soon become apparent, this phase angle is strictly bounded to $0 < \theta < \frac{\pi}{2}$ under conditions of dynamic equilibrium.

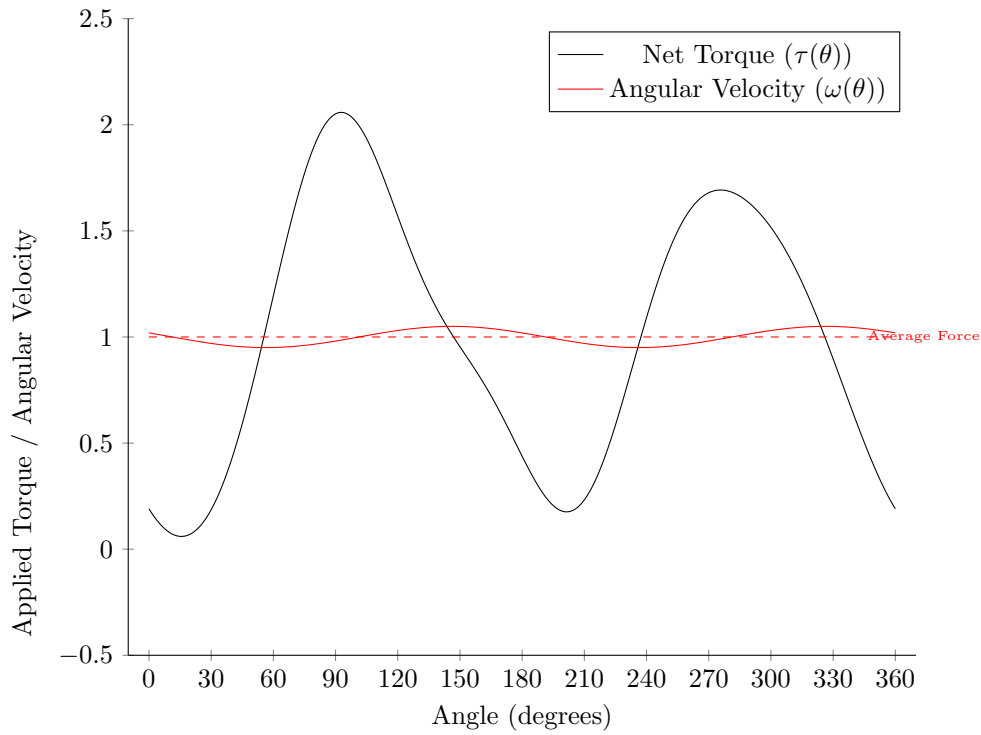


Figure 7: Variations in Applied Torque and Angular Velocity

The following section will develop the mathematical relationship between applied torque and induced angular velocity. relates to applied torque.

3.5 System Modelling

A cyclist under dynamic equilibrium faces a net impeding force that is a function of their velocity. If a linear approximation of these resistive forces is used, then the BRS to be modelled as a mass-damper system as shown in Figure 8.

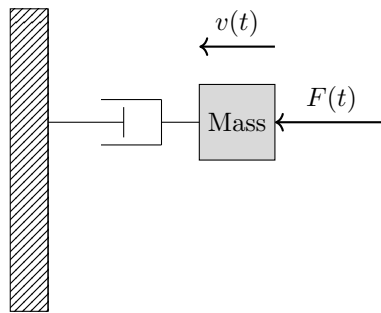


Figure 8: Mass-Damper Model of a Cyclist

Sources of impedance (to movement) can be replaced with their electrical analogues (Inductance for Mass, and Resistance for Friction and Wind Resistance). Extending the analogy, the Force applied by the system (which is transferred from pedal force) is represented by Voltage, and the resultant Current represents Velocity. This is represented in Figure 9 below - V represents the applied force, and V_g represents the constant opposing force due to gravity.

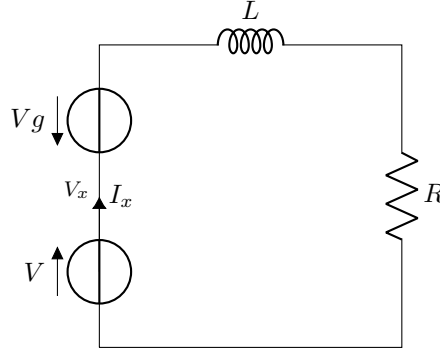


Figure 9: General Circuit Model of a BRS

The value of resistance is as follows

$$R = \frac{F_d(v)}{v} \quad (14)$$

Consider $v(t)$, representing the force applied by the cyclist over time, to be a Fourier Series:

$$v(t) = v_0 + \sum_{n=1}^{\infty} v_n \sin(2\pi n t + \phi_n) \quad (15)$$

In the frequency domain, the Reactive Impedance seen by the n_{th} harmonic is given by:

$$X_n = j\omega n L \quad (16)$$

Taking a phasor representation of that particular harmonic (phasor quantities are RMS, and denoted with capital letters), the n_{th} harmonic current induced in the circuit resulting from the applied harmonic voltage is given as:

$$I_{x,n} = \frac{V_{x,n}}{X_n + R} \quad (17)$$

By the principle of superposition, the total current in the circuit is the sum the current contributions of individual harmonics, so total current in the circuit can also be expressed as a Fourier Series:

$$i(t) = i_0 + \sum_{m=1}^{\infty} i_m \sin(2\pi m t + \phi_m) \quad (18)$$

Now consider the computation of the power dissipated by the resistor over one period of the fundamental frequency (T). First note the following, via an application of the general fact established in Equation 12:

$$P_{avg} = \frac{1}{T} \int_0^T V(t)I(t) dt \neq \frac{1}{T} \int_0^T V(t) dt * \frac{1}{T} \int_0^T I(r) dt$$

If there is in fact greater or lesser power produced in reality (as measured by IAV) than is computed via AAV, this negative *Power Error* represents power dissipated into the wind and to other frictional forces by the cyclist due to oscillations¹². The following section will characterise harmonic losses in RL circuits in terms of the interaction between the various harmonics.

3.5.1 Harmonic Losses in RL Circuits with multiple harmonics and a DC Offset

Over a single period (normalised to 1 second), the energy dissipated by a resistor in an RL circuit with periodic and incoherent voltage source is given by:

$$\int_0^1 v(t) * i(t) dt = \int_0^1 (v_0 + \sum_{n=1}^{\infty} v_n \sin(2\pi n t + \phi_n)) * (i_0 + \sum_{m=1}^{\infty} i_m \sin(2\pi m t + \psi_m)) dt = v_0 i_0 \pm \epsilon \quad (19)$$

Where $v_0 i_0$ is the power dissipated by the DC components of voltage and current, and ϵ is the power dissipated by harmonics. Note the following lemmas for $n, m \in \mathbb{N}$ where $n \neq m$ and $\phi_n, \phi_m \in \mathbb{R}$:

$$\int_0^1 \sin(2\pi n t + \phi) dt = 0 \quad (20)$$

¹²Positive Power Error would indicate external forces performing harmonic work on the BRS

$$\int_0^1 \sin(2\pi nt + \phi) * \sin(2\pi nt + \phi + \frac{\pi}{2}) dt = 0 \quad (21)$$

$$\int_0^1 \sin(2\pi nt + \phi_n) * \sin(2\pi mt + \phi_m) dt = 0 \quad (22)$$

The integrand of Equation 19 can be expanded binomially, yielding five distinct terms:

$$\int_0^1 v_0 * i_0 dt = 0 \quad (23)$$

$$\int_0^1 (\sum_{n=1}^{\infty} v_n \sin(2\pi nt + \phi_n)) * (i_0) dt = 0 \quad (24)$$

$$\int_0^1 (v_0) * (\sum_{k=1}^{\infty} i_k \sin(2\pi kt + \psi_k)) dt = 0 \quad (25)$$

$$\int_0^1 \sum_{n=1}^{\infty} (v_n \sin(2\pi nt + \phi_n)) * (i_n \sin(2\pi nt + \psi_n)) dt \quad (26)$$

$$\int_0^1 \sum_{n=1}^{\infty} \sum_{k=1, k \neq n}^{\infty} (v_n \sin(2\pi nt + \phi_n)) * (i_k \cos(2\pi kt + \psi_k)) dt = 0 \quad (27)$$

By the fact of Lemma 20, Equations 24 and 25 evaluate to zero. By the fact of Lemma 22, Equation 27 evaluates to zero. By the fact of Lemma 21, Equation 26 evaluates to zero when harmonics of the same order are in quadrature. Therefore, the only contribution to ϵ derives from harmonics of the same order that are not in quadrature. This can be computed as follows:

$$\epsilon = \sum_{n=1}^{\infty} \Re(V_{x,n} * I_{x,n}) = \sum_{n=1}^{\infty} \frac{|V_{x,n}|^2}{|j\omega nL + R|} \cos(\tan^{-1}(\frac{R}{j\omega L})) \quad (28)$$

Note that ϵ is strictly positive, and this is due to the fact that resistance must take on a positive value.

3.5.2 Unilateral Torque Measurement

Torque application is unilateral¹³, and may be measured unilaterally, however angular acceleration is a function of net torque. Extending the electrical analogy, power produced unilaterally can be expressed as two individual voltage sources, each with a characteristic harmonic profile:

$$v_l(t) = v_{l,0} + \sum_{n=1}^{\infty} v_{l,n} \sin(2\pi nt + \phi_n)$$

$$v_r(t) = v_{r,0} + \sum_{n=1}^{\infty} v_{r,n} \sin(2\pi nt + \psi_n)$$

As shown in Figure 10, voltage sources are arranged head-to-tail, and result in a certain node voltage, which represents the net torque/voltage; it is the net voltage at this node which induces a current in the circuit. The net voltage can then be expressed as a time-domain summation:

$$v_x(t) = v_l(t) + v_r(t) = v_{x,0} + \sum_{n=1}^{\infty} v_{x,n} \sin(2\pi nt + \delta_n) \quad (29)$$

Phasor Representation for a particular harmonic (n) is possible for for the Left($V_{l,n}$), Right($V_{r,n}$) and Net($V_{x,n}$) Voltages, and for net current $I_{x,n}$. Unilateral power error can be computed as follows:

$$P_l = \sum_{n=1}^{\infty} \Re(V_{l,n} * I_{x,n}) \quad (30)$$

$$P_r = \sum_{n=1}^{\infty} \Re(V_{r,n} * I_{x,n}) \quad (31)$$

¹³That is, torque is applied by both feet to the crankarms independently, which produces a resultant net torque on the crankarm

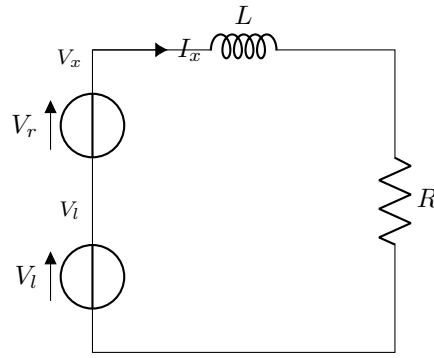


Figure 10: Circuit Model of a Cyclist Producing Unilateral Torque

In Table 2, it is clear that the magnitude of the first harmonic of torque as measured on the left and right crankarms is substantially higher than the magnitude of net torque; it is also obvious that there is phase displacement of left and right torque with respect to net torque. We might thus predict the presence of spurious power error if unilateral power was measured.

3.5.3 A Tangential Comment on Dynamic Inequilibrium

Under conditions of Dynamic Inequilibrium, initial velocity does not equal terminal velocity. This introduces a DC Term $F(t)$ which could take an arbitrary form, represented in Figure 11.

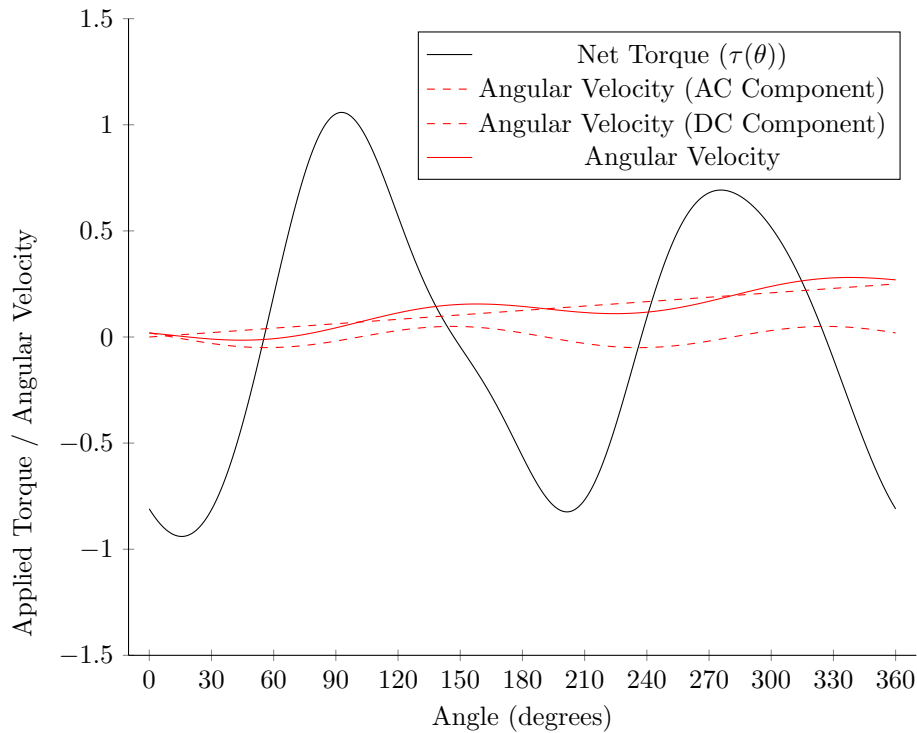


Figure 11: Variations in Applied Torque and Angular Velocity - Dynamic Inequilibrium

The resultant error essentially derives from the extent to which the DC component deviates from linearity.

4 Model Validation and Extrapolation

The purpose of this section is to numerically test the model developed in Section 3 against the subset of results from Favero’s Paper as shown in Table 5, and then to use the model to predict scenarios where Power Error might occur beyond the scenarios tested experimentally. The model essentially encodes the dynamic model of a cyclist developed above, and computes power error by taking the following inputs:

v as the linear velocity of the bicycle-rider system with respect to the ground.

v_{wind} as the average velocity of the wind with respect to the ground.

m as the mass of the entire bicycle-rider system. This value was estimated at 75kg for a cyclist riding outdoors, and 3kg for an indoor trainer.

g as the gravitational constant.

$\frac{1}{2}\rho C_d A$ is used to determine drag. For a cyclist riding outdoors, this was estimated to be $0.25m^2$, and a higher value of $0.5m^2$ was used for the indoor trainer.

Cadence is the rate at which the pedal performs a full revolution about the bottom bracket.

HarmonicProfile as per Table 2

The model computes Resistance according to Equation 14. AAV is computed according to Equation 6. Power Error is computed according to Equation 28, and Unilateral Power Errors for left and right are computed according to Equations 30 and 31. Variation is computed according to:

$$Var(\%) = \frac{\sqrt{\sum_{n=1}^{\infty} (2 * V_x)^2}}{v} \quad (32)$$

The developed model is sensitive to input parameters, many of which are unknown (such as actual mass, actual harmonic profile, actual drag). This may explain the deviation between model results and experimental data.

4.0.1 Model Fidelity

For each scenario enumerated in Table 3, a velocity was chosen for v of Table 4 (to one DP of precision) that most closely matched the resultant power value from P_{target} of Table 3. It should be noted that simulated AV Variation was generally lower than measured. This could be due to a number of experimental factors such as measurement noise, or deviation from Dynamic Equilibrium. There were no conditions where Power Error (ϵ_x) was significant ($> 0.25\%$), however unilateral power error reached as high as 0.42%. It can be concluded that, in high inertia scenarios, any power error indicated in Favero’s Paper cannot be attributed to the interaction of harmonics of torque and angular velocity within the pedal stroke.

#	Name	Mass (kg)	$\frac{1}{2}\rho C_d A$ (m^2)	Cadence (rpm)	P_{target} (W)	Var_{target} (%)	ϵ_{target}
Outdoors							
1	Flat Ground, 100rpm	75	0.25	100	192.08	6.2	0.04
2	Flat Ground, 90rpm	75	0.25	90	212.90	6.7	0.10
3	5% Grade ¹⁴	75	0.25	60	295.16	8.1	0.48
Trainer ¹⁵							
4	70% FTP 90rpm	4	0.5	90	230.26	4.8	-0.36
5	70% FTP 110rpm	4	0.5	110	213.18	4.2	-0.22
6	95% FTP 90rpm	4	0.5	90	287.24	6.3	-0.51
7	95% FTP 70rpm	4	0.5	70	270.14	8.0	-0.86
Synthetic Scenarios							
8	10% Grade	75	0.25	50	-	-	-
9	15% Grade	75	0.25	40	-	-	-
10	Strong Headwind	75	0.25	70	-	-	-

Table 3: Scenario Definitions

¹⁴No cadence value was provided in Favero’s Paper, so an average cadence of 60rpm was assumed

¹⁵Trainer resistance is assumed to be higher than the equivalent outdoor resistance

#	v (ms^{-1})	v_{wind} (ms^{-1})	P (W)	Var (%)	ϵ_x	ϵ_l	ϵ_r
1	9.2	0.0	194.67	0.13	0.00	-0.01	0.01
2	9.5	0.0	214.34	0.15	0.00	-0.01	0.01
3	6.3	0.0	294.27	0.69	0.00	-0.06	0.06
4	7.7	0.0	228.43	4.46	0.07	-0.21	0.40
5	7.5	0.0	211.08	4.35	0.07	-0.21	0.39
6	8.3	0.0	286.05	3.94	0.06	-0.20	0.35
7	8.2	0.0	275.90	4.75	0.08	-0.21	0.42
8	5.0	0.0	430.38	1.92	0.00	-0.17	0.17
9	3.0	0.0	344.60	5.34	0.00	-0.47	0.47
10	3.0	15.0	486.32	4.29	0.07	-0.21	0.38

Table 4: Simulation Parameters

4.1 Simulations

There was a degree of uncertainty in relation to the particular parameters chosen to recreate the experimental results from Favero's Paper. To strengthen the claims made by this paper, 260'000 simulations were performed which capture all plausible riding scenarios. Simulations with power values above 600w were excluded. The input parameters were varied in the following fashion:

1. **Mass**, from 1kg to 10kg in increments of 1kg (representing indoor trainer flywheel mass), and from 10kg to 90kg in increments of 5kg.
2. **Cadence**, from 40rpm to 120rpm in increments of 10rpm.
3. **Gradient**, from 0% to 20% in increments of 1%.
4. **Velocity**, $1ms^{-1}$ to $15ms^{-1}$ in increments of $1ms^{-1}$.
5. $\frac{1}{2}\rho CdA$ **Values**, from $0.25m^2$ to $0.5m^2$ in increments of $0.05m^2$.

4.1.1 AV Variation and Power Error

Results were separated into low and high inertia contexts. High inertia contexts correspond to situations where a cyclist is riding outdoors. It is obvious there are no plausible high inertia scenarios where any degree of power error is present, even when AV Variation is extremely high. When AV Variation is high, indicating a very high second harmonic of AV, the phase relationship between torque and AV is such that no real work is done by the interaction of the harmonics of torque and AV.

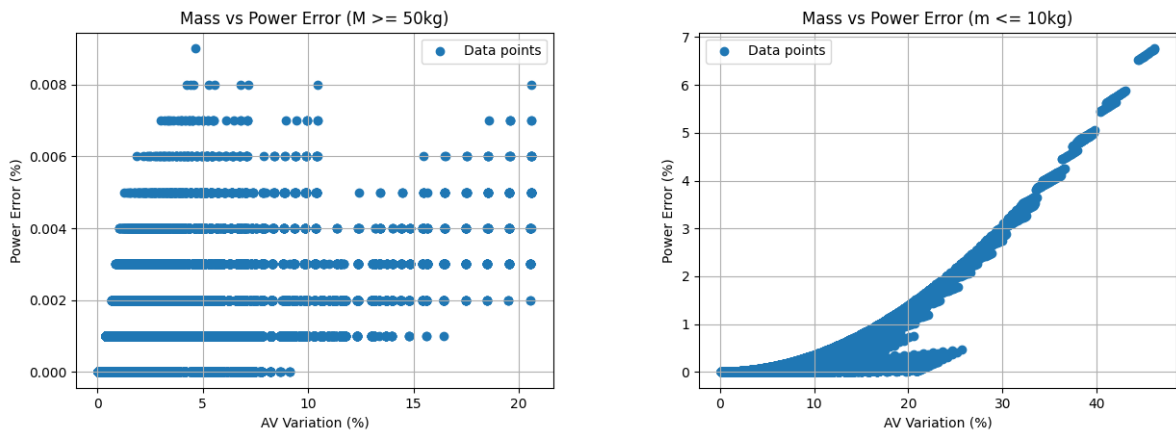


Figure 12: Power Error and AV Variation

Favero's Paper did in fact note high power error. Recall that power was measured unilaterally. High levels of unilateral power error do in fact occur under simulation, as shown in Figure 13, and there is a very strong relationship between AV Variation and Unilateral Power Error. Note the complementarity of power error; high left power error is negated by high right power error in the opposing direction. The relationship between AV Variation and Unilateral Power Error is stronger under simulation than experimentally. This could be due to measurement noise, or rider deviation from Dynamic Equilibrium. The final consideration is that observed

Power Error in the high inertia contexts in Table 3 have a positive sign; AAV overpredicts power. This is a physical impossibility for genuine power error based on simulation results and the model developed above. Thus, the most likely explanation for observed power error from Favero's Paper is as a spurious artefact of experimental design; namely, the unilateral measurement of power.

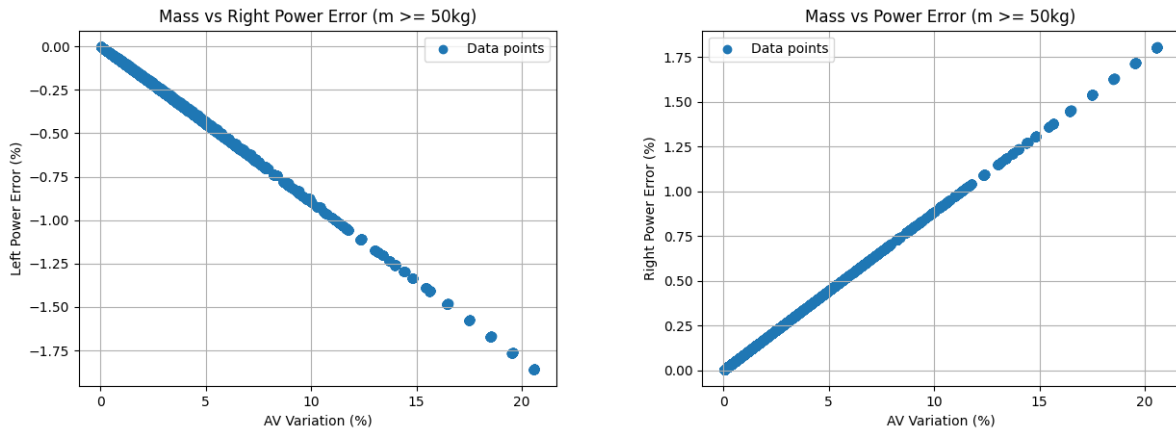


Figure 13: L/R Power Error and AV Variation

AV Variation is a poor predictor of Power Error, however Mass and Cadence clearly have a relationship to Power Error. As can be seen in Figure 14.

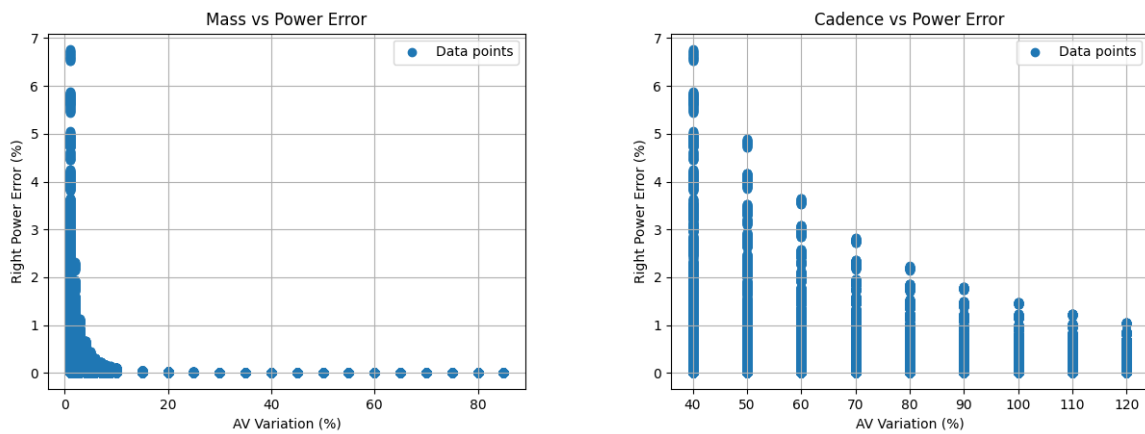


Figure 14: Relationship between Mass, Cadence and Power Error

5 Conclusion

Theoretical analysis and simulation results indicate that power error resulting from the interplay of torque and angular velocity harmonics within a pedal stroke does not occur to any meaningful extent in high inertia scenarios. Furthermore, there is no direct relationship between variation in Angular Velocity and Power Error under conditions of Dynamic Equilibrium. This undermines the fundamental claims made by Favero in their paper. This paper notes the strong likelihood of a flaw in Favero's experimental methodology, and strongly encourages Favero to perform a revised experiment accounting for bilateral power - this paper hypothesises that Favero will observe a substantially lower magnitude of power error under most circumstances where circular chainrings are used.

It should be noted that the claims of this paper are modest; it is certainly possible that IAV could outperform AAV under conditions that fall beyond the scope of this paper, which assumed Dynamic Equilibrium and the perfect transmission of power from the pedal to the rear wheel.

References

- [1] Rodrigo R Bini, Felipe P Carpes, et al. *Biomechanics of cycling*. Springer, 2014.
- [2] Tomasz Danek, Michael A. Slawinski, and Theodore Stanoev. On modelling bicycle power-meter measurements: Part ii. relations between rates of change of model quantities, 2020.
- [3] Favero. Influence of angular velocity of pedaling on the accuracy of the measurement of cyclist power, 2018.

Annex A - Subset of Favero Tests

id	Mass (kg) ¹⁶	Gradient (%)	Cadence (rpm) ¹⁷	AV Var (%)	IAV (W)	AAV (W)	ϵ (%)
1	4	0	90	4.8	258.5	257.4	-0.42
2	4	0	90	4.3	180.6	180.7	0.04
3	4	0	90	6.1	261.3	259.4	-0.71
4	4	0	90	3.1	216.1	215.6	-0.23
5	4	0	90	5.6	234.8	233.7	-0.49
6	4	0	110	3.8	225.6	225.4	-0.11
7	4	0	110	4.1	188.7	189.0	0.16
8	4	0	110	4.3	256.2	255.1	-0.43
9	4	0	110	2.6	172.8	172.7	-0.06
10	4	0	110	6.1	222.6	221.1	-0.66
11	4	0	90	5.6	306.8	305.3	-0.51
12	4	0	90	5.6	264.1	263.8	-0.09
13	4	0	90	7.3	326.3	322.6	-1.15
14	4	0	90	3.9	276.6	276.0	-0.21
15	4	0	90	6.2	262.7	261.2	-0.57
16	4	0	70	7.4	286.0	283.8	-0.76
17	4	0	70	10.0	234.1	232.1	-0.82
18	4	0	70	10.3	335.4	330.0	-1.59
19	4	0	70	6.5	261.1	259.9	-0.47
20	4	0	70	7.6	234.1	232.6	-0.64
21	65	0	100	5.0	205.8	205.9	0.07
22	71	0	100	6.0	161.3	161.2	-0.10
23	68	0	100	5.4	245.7	246.0	0.11
24	67	0	100	4.4	168.8	169.0	0.15
25	62	0	100	10.1	178.8	178.8	-0.04
26	65	5	60	7.8	331.4	332.5	0.34
27	71	5	60	10.0	268.9	270.1	0.45
28	68	5	60	8.0	357.2	259.4	0.62
29	67	5	60	6.9	258.8	260.4	0.63
30	62	5	60	7.9	259.5	260.3	0.31
31	65	5	90	5.9	241.6	241.9	0.11
32	71	5	90	6.5	215.1	215.1	-0.02
33	68	5	90	5.0	262.1	262.6	0.20
34	67	5	90	4.7	165.8	165.9	0.06
35	62	5	90	11.6	179.9	180.1	0.13

Table 5: Subset of Favero Tests

	Mass	Grade	RPM	Var	IAV	AAV	Force	FMR	E	E2
Mass	-	0.00	0.23	0.11	0.35	0.18	0.64	0.00	0.00	0.02
Grade	0.00	-	0.00	0.05	0.43	0.68	0.02	0.00	0.00	0.30
RPM	0.23	0.00	-	0.00	0.00	0.00	0.00	0.68	0.60	0.01
Var	0.11	0.05	0.00	-	0.09	0.13	0.00	0.89	0.46	0.01
IAV	0.35	0.43	0.00	0.09	-	0.00	0.00	0.02	0.14	0.00
AAV	0.18	0.68	0.00	0.13	0.00	-	0.00	0.00	0.04	0.00
Force	0.64	0.02	0.00	0.00	0.00	0.00	-	0.29	0.98	0.00
FMR	0.00	0.00	0.68	0.89	0.02	0.00	0.29	-	0.00	0.00
E	0.00	0.00	0.60	0.46	0.14	0.04	0.98	0.00	-	0.00
E2	0.02	0.30	0.01	0.01	0.00	0.00	0.00	0.00	0.00	-

Table 6: Subset P-Values

¹⁶An estimate of 4kg was taken to represent the equivalent inertia of the Elite Quobo Magnetic Flywheel. Mass is as provided in Favero, and does not include the mass of the bicycle, clothes, etc (which is usually taken to be 10kg)

¹⁷Cadence was not provided for the climbing segment, so an estimate of 60rpm was taken